Published in final edited form as:

Protein Expr Purif. 2017 July ; 135: 45–53. doi:10.1016/j.pep.2017.04.010.

Overexpression of Ebola virus envelope GP1 protein

Zhongcheng Zou[a], **John Misasi**[b], **Nancy Sullivan**[b], and **Peter D. Sun**[a,*]

[a]Structural Immunology Section, Laboratory of Immunogenetics, National Institute of Allergy and Infectious Diseases, National Institutes of Health, Rockville, MD 20852, USA

[b]Biodefense Research Section, Vaccine Research Center, National Institute of Allergy and Infectious Diseases, National Institutes of Health, Bethesda, MD 20892, USA

Abstract

Ebola virus uses its envelope GP1 and GP2 for viral attachment and entry into host cells. Due to technical difficulty expressing full-length envelope, many structural and functional studies of Ebola envelope protein have been carried out primarily using GP1 lacking its mucin-like domain. As a result, the viral invasion mechanisms involving the mucin-like domain are not fully understood. To elucidate the role of the mucin-like domain of GP1 in Ebola-host attachment and infection and to facilitate vaccine development, we constructed a GP1 expression vector containing the entire attachment region (1–496). Cysteine 53 of GP1, which forms a disulfide bond with GP2, was mutated to serine to avoid potential disulfide bond mispairing. Stable expression clones using codon optimized open reading frame were developed in human 293-H cells with yields reaching ~25 mg of GP1 protein per liter of spent medium. Purified GP1 was functional and bound to Ebola attachment receptors, DC-SIGN and DC-SIGNR. The over-expression and easy purification characteristic of this system has implications in Ebola research and vaccine development. To further understand the differential expression yields between the codon optimized and native GP1, we analyzed the presence of RNA structural motifs in the first 100 nucleotides of translational initiation AUG site. RNA structural prediction showed the codon optimization removed two potential RNA pseudoknot structures. This methodology is also applicable to the expression of other difficult virus envelope proteins.

Keywords

Ebola; Virus; GP1; Protein expression and purification

1. Introduction

Ebola virus is an enveloped negative-stranded RNA virus and belongs to the Filoviridae family. There are currently five species of Ebola virus: Reston, Tai Forest, Sudan, Zaire, and Bundibugyo Ebola virus. Ebola virus is the etiological agent of Ebola virus disease, and has drawn considerable attention since its discovery in 1976 due to devastating human outbreaks in Africa, as well as its suitability as a biological weapon [1]. Ebola virus infection results in

*Corresponding author. Structural Immunology Section, Laboratory of Immunogenetics, National Institute of Allergy and Infectious Diseases, National Institutes of Health, 12441 Parklawn Drive, Rockville, MD 20852, USA. psun@nih.gov (P.D. Sun).

severe hemorrhagic fever leading to multiple organ failure and high mortality. There are no effective vaccines approved for widespread prophylactic use to date, and current treatments consist primarily of palliative care [2,3].

Ebola virus infects many cell types, although its primary targets are monocytes, macrophages, and dendritic cells (DCs) [4], suggesting multiple cell-surface receptors can facilitate viral attachment and entry. The list of receptors implicated in Ebola infection include C-type lectins (CLEC4L, CLEC4M, CLEC4G, CLEC10A, CLEC6A, and MBL2) [5,6], folate receptor [7], Rho GTPases [8], β1-integrins [9], and TIM/TAM receptors [10,11]. Other molecules, such as heparan sulfate, heparin, and other glycosaminoglycans are also reported to promote viral attachment [12–14].

The Ebola virus genome contains seven genes which direct the synthesis of eight proteins. Transcriptional editing of the fourth gene results in expression of a 676-residue transmembrane-linked envelope glycoprotein termed GP, as well as a 364-residue secreted glycoprotein termed sGP [15,16]. GP is a ‘class I’ viral membrane fusion glycoprotein that forms a homotrimer on the surface of virions and resembles the prototypic HIV-1 Env and influenza virus hemagglutinin (HA) in overall organization. GP is necessary and sufficient to mediate Ebola virus entry into the cytoplasm of host cells [17]. It is expressed as a precursor that is cleaved at residue 501 to yield two subunits: GP1 and GP2, which remain linked by a di-sulfide bond [18]. The membrane-distal subunit, GP1, contains the putative receptor-binding region, as well as two heavily glycosylated domains: a glycan cap which sits immediately atop the putative receptor-binding site and a larger, mostly unstructured mucin-like domain that contains a dense clustering of N- and O-linked glycans (Fig. 1). GP1 plays a key role in viral attachment and entry and therefore is a target for both vaccine development and therapeutic treatment. Following the initial attachment of virions to the host cell surface, Ebola virus is thought to be internalized to endosomes/lysosomes (LE/LYs) via macropinocytosis, whereby GP is cleaved by host cysteine proteases to generate a ligand for Niemann-Pick C1 (NPC1), a multi-membrane spanning cholesterol transport protein in LE/Lys [19]. While pseudotyped viruses lacking the mucin-like domain are infectious in cell culture [20], the mucin-like domain has been proposed to mediate viral adhesion to specific cell types and contribute to viral immune evasion through shielding neutralization epitopes [21,22]. Shorter fragments of GP1 lacking the mucin domain have been expressed [23,24], but the attempt to express full-length GP1 has proven difficult [25]. To elucidate the GP1 mucin-like domain function and facilitate vaccine development, we expressed a full-length *Zaire Ebola* GP1, including the mucin-like domain. Our expression system yielded greater than 20 mg of GP1 from 1 L of spent medium.

2. Materials and methods

2.1. Antibodies and proteins—Mouse anti-Zaire GP monoclonal antibody, clone 6D8 (mAb6D8), known to bind a linear epitope in mucin-like domain [26], was kindly provided by Dr. John Dye of US Army Medical Research Institute of Infectious Diseases. Conformation-dependent Ebola-specific monoclonal antibodies (mAb114, mAb13C6, and mAb100) were produced recombinantly using transient transfections [27]. mAb114 binds to a conformational epitope in the core region of GP1 and acts by blocking receptor binding to

GP. mAb 13C6 makes conformation-dependent contacts within the glycan cap region of GP1. mAb100 binds to the base of GP, primarily making conformation-dependent contacts with GP2 [26–30]. Fab fragments were obtained by binding monoclonal antibodies containing an HRV3C protease site in the hinge region to a protein A column and digesting with HRV3C protease (Novagen, Madison, WI) as described previously [27]. Trimeric Ebola virus GP protein lacking the mucin like domain (GPΔMuc) prepared from 293 cells was also described previously [27].

2.2. Plasmid construction

Two GP1 expressing vectors, pcDNA-nGP1 and pcDNA-oGP1, were constructed. Both vectors encode the *Zaire Ebola virus* GP1 (amino acid residues from 1 to 496), an AviTag (GLNDI-FEAQKIEWHE) and a six-histidine tag at the C-terminus. A BamHI restriction enzyme site was inserted between GP1 and AviTag. Cys 53 of GP1, which forms a disulfide with Cys 609 from GP2, was mutated to Ser to avoid mispairing of disulfides. Both the native sequence (nGP1) and that of a codon optimized (oGP1) sequence using OptimumGene™ Codon Optimization Analysis tool from GenScript (Piscataway, NJ) were synthesized and cloned into pcDNA3.1 (+) vector (Invitrogen, Carlsbad, CA) between NheI and NotI sites.

2.3. Transient and stable expression of GP1

293T or 293-H cells (Invitrogen) were grown in DMEM/F12 medium containing 5% FBS. For transient expression, a T-25 flask was seeded with 1×10^6 293T cells one day before the transfection. Six μg of pcDNA-nGP1 or pcDNA-oGP1 was diluted into 0.3 ml OPTI-MEM I reduced serum medium and 24 μl of FuGENE® HD Transfection Reagent (Promega, Madison, WI) was then added into the solution. The transfection reagent and DNA mix was incubated for 20 min at room temperature, then added into the T-25 flask. The medium was replaced after 24 h and cells were cultured continuously for another 5 days. Supernatants were then taken for an ELISA expression test. To establish a stable GP1 expressing cell line, 293-H cells were transfected in the same way with pcDNA-oGP1 plasmid, then seeded into 384-well plates and cultured with DMEM/F12 medium containing 5% FBS and 500 μg/ml G418 two days post transfection. After approximately two weeks, colonies were screened for their GP1 expression by ELISA. Briefly, 1 μg of mAb6D8 antibody was immobilized onto each well of an ELISA plate. Horseradish peroxidase labeled rabbit anti-6X His tag polyclonal antibody (Abcam, Cambridge, MA) was used as a detection antibody with a dilution of 1/5000. The clone with the highest expression level of GP1 was chosen for recombinant protein production.

2.4. Recombinant GP1 preparation

The top GP1-expressing clone was expanded in T-500 triple layer flasks in DMEM/F12 medium supplemented with 5% FBS and 500 μg/ml G418. When the cultures reached confluence, cells were washed with Hank's solution and cultured with serum-free 293 Expression Medium (Invitrogen) for one week. The spent medium was filtered with a 0.22 μm filter and loaded onto a 20 ml Ni Sepharose column in the presence of 20 mM of imidazole. Eluted protein fractions were dialyzed against PBS or 50 mM Tris-HCl, pH 7.0 buffers. Protein concentration was determined by using a Bicinchoninic Acid (BCA) protein

assay kit (Sigma-Aldrich, St. Louis, MO). SDS-PAGE was performed using NuPAGE™ Novex™ 4–12% Bis-Tris polyacrylamide gels (Invitrogen) under reducing or nonreducing conditions. For Western blot analysis, SDS–PAGE gel-separated proteins were transferred onto polyvinylidene difluoride (PVDF) membranes (Millipore, Billerica, MA), blotted with 5 μg/ml of mAb6D8 and a secondary goat anti-mouse IgG antibody conjugated with horseradish peroxidase (Sigma-Aldrich) at 1:20000 dilution. The peroxidase substrate was TMB 1-Component Membrane Peroxidase Substrate (KPL, Inc., Gaithersburg, MD).

2.5. Binding measurements by BIAcore 3000, Fort eBio Octet HTX, and ELISA

Surface plasmon resonance (SPR) measurements were performed using a BIAcore 3000 instrument (BIAcore, Uppsala, Sweden). Purified GP1 protein was immobilized on a flow cell of a CM5 sensor chip at a concentration of 10 μg/ml in 50 mM sodium acetate, pH 5.0, using *N*-hydrosuccinimide/1-ethyl-3-(3-dimethylaminopropyl)-carbodiimide hydrochloride (NHS/EDC) at a flow rate of 10 μl/min. Binding of mAb6D8 to the immobilized GP1 was measured using serial dilutions of the antibody from 40 to 0.078 μg/ml at a flow rate of 20 μl/min in PBS.

Binding of recombinant GP1 to mAb114, mAb13C6 and mAb100 were performed using a ForteBio Octet HTX instrument using AR2G biosensors (amine-reactive 2nd generation) or anti-human Fc biosensors (ForteBio, Menlo Park, CA). A mucin-like domain deleted envelope, GPΔMuc, was used as a comparison. In experiments using the AR2G biosensors, sensors were activated by a mixture of EDC and NHS (diluted in water at 3.75 and 1.15 mg/ml, respectively) for 300 s. Sensors were loaded with 10 μg/ml of GPΔMuc in 10 mM Acetate (pH4.5) or 10–15 μg/ml of GP1 in 10 mM Acetate (pH5.5) for 600–1500 s. Typical capture levels after quenching with 1M ethanolamine (pH 8.0) for 300 s were between 1.0 and 2.9 nm, and variability within the same protein did not exceed 0.3 nm. Bio-sensors were then equilibrated for 300 s in PBS +1% BSA +0.01% Tween-20+ 0.02% sodium azide (PBS-BSA) prior to binding assessment of the Fabs. Association of Fabs (400–6.25 nM in PBS-BSA) was measured for 300 s and dissociation was measured for 300–1200 s in PBS-BSA. All the assays were performed with agitation set to 1000 rpm at 30 °C. Correction to subtract nonspecific baseline drift was carried out by subtracting the measurements recorded for a sensor loaded with HIV-1 gp120 incubated with the Fabs. In experiments measuring GP1 binding to intact monoclonal antibodies, anti-human Fc biosensors were loaded for 600 s with 10 μg/ml monoclonal antibodies diluted in PBS-BSA. Biosensors were then equilibrated for 60 s in PBS-BSA prior to binding assessment of monomeric GP1 protein (400–6.25 nM in PBS-BSA) for 300 s. Dissociation was measured for 300–1500 s in PBS-BSA. Correction to subtract non-specific was carried out by subtracting the measurements recoded for sensors loaded with an isotype control antibody or a non-specific ligand (HIV-1 gp120). Data analysis and curve fitting were carried out using Octet analysis software, version 9.0. Experimental data were fitted using a 1:1 binding model. Global analyses of the complete data sets assuming binding was reversible (full dissociation) were carried out using nonlinear least-squares fitting allowing a single set of binding parameters to be obtained simultaneously for all concentrations used in each experiment.

DC-SIGN or DC-SIGNR binding to the GP1 and GPΔMuc were assayed using ELISA method in which GP1 or GPΔMuc in 10 mM Tris buffer, pH 8.0 was coated on a 96-well ELISA plate at a concentration of 10 μg/ml. After blocking, DC-SIGN or DC-SIGNR Fc fusion proteins (R&D systems, Minneapolis, MN) were added into the plate followed by horseradish peroxidase-conjugated mouse anti-human IgG Fc antibody (Sigma-Aldrich). All the buffers used for ELISA contained 2 mM of $CaCl_2$.

2.6. Deglycosylation and biotinylation of GP1 protein

To remove GP1-associated sialic acids, purified GP1 protein was treated with 0.5 U/mL of neuraminidase from Arthrobacter ureafaciens (Roche Diagnostics, Chicago, IL) in acetate buffer, pH 5.5 at 37 °C for 2 h. After treatment, the sample pH was restored to neutral. For N-linked glycan removal, GP1 protein in denaturing buffer was first denatured by incubation at 100 °C for 10 min, PNGase F (New England Biolabs, Beverly, MA) was then added and digestion was performed at 37 °C for 2 h. Treated or untreated samples were then analyzed by Western blot under reducing conditions.

GP1 was biotinylated using a BirA biotin-protein ligase standard reaction kit (Avidity LLC, Aurora, CO) according to the manufacture's protocol. Briefly, purified GP1 protein was buffer exchanged to 10 mM Tris buffer, pH 7.5. BiomixA (100 μl), BiomixB (100 μl), and BirA ligase (13 μg) were added into 800 μl of GP1 (6.25 mg/ml). After mixing, the sample was incubated at room temperature for 1.5 h and then dialyzed against 10 mM Tris buffer, pH 7.5. The extent of GP1 biotinylation was examined by biotinylation reaction titration assay.

2.7. Cell-surface binding analysis

The staining and wash buffer was Hanks' Balanced Salt Solution with 3% FBS, 2 mM $CaCl_2$ and 0.1% NaN_3 added. Cells were blocked with 5% FBS first and then incubated with biotinylated GP1 for 30 min. After washing three times, cells were stained with PE-conjugated streptavidin (R&D Systems) for 30 min. All incubations were carried out on ice. Analyses were performed using a Becton-Dickinson FACS Calibur flow cytometer (BD Biosciences, San Jose, CA).

3. Results

3.1. GP1 protein expression and purification

Recombinant Ebola virus envelope protein is difficult to express at high levels. It is possible that the native DNA sequence is not optimal for expression. In this work, two GP1 expression vectors, pcDNA-nGP1 and pcDNA-oGP1, which contained the full-length (amino acids 1–500) native and optimized GP1 sequence respectively, were constructed for comparison (Fig. 1). The optimization was performed using Genescript's OptimumGene™ Codon Optimization Analysis tool that was mainly based on human cell codon usage bias and GC content. A 15-amino acid AviTag followed by a six-histidine tag was fused to the C-terminus of GP1.

To compare potential DNA effects on GP1 expression levels, pcDNA-nGP1 and pcDNA-oGP1 were used to transfect 293T cells. Transient expression results showed that GP1 expression using optimized DNA was ~3 fold higher than that by native sequence (Fig. 2), indicating optimization increased the expression level. Based on this result, pcDNA-oGP1 was used to transfect 293-H cells to establish stable GP1 expressing cell lines. After transfection, more than two hundred G418 resistant clones were screened for their GP1 expression levels. Clone 109 expressed the highest level of GP1 and was expanded in T500 flasks. Upon confluency, the selection medium was replaced with serum-free medium and culture continued for about a week to allow accumulation of GP1. The concentration of GP1 in harvest reached 25 mg/L as determined by ELISA. Harvest medium was loaded onto a Ni-Sepharose column and proteins were then eluted with a linear concentration gradient of imidazole. After only one step of purification, about 20 mg of GP1 protein was obtained from 1 L of spent medium.

3.2. Characterization of purified GP1 protein

The recombinant GP1 exhibited as a single peak on a size exclusion chromatography elution profile (Fig. 3A) and an 80–160 kD glycosylated protein band on a ProBlue (National Diagnostics, Atlanta, GA) stained SDS-PAGE gel (Fig. 3B). The purified protein was confirmed to be GP1 by N-terminal peptide sequencing, and was reactive to GP1-specific antibodies by western blot and BIAcore (Fig. 3C and D). GP1 is a heavily glycosylated protein, containing 15 N-linked and multiple O-linked glycosylation sites. To analyze the glycan composition, we treated the protein with neuraminidase and PNGase F, which removed sialic acid and most of N-linked carbohydrates respectively. Western blot showed that neuraminidase treated GP1 migrated visibly faster than untreated GP1, indicating the presence of significant amount of sialic acid. PNGase F digestion reduced the molecular weight of GP1 from 80 to 160 kD to 65–120 kD (Fig. 3E), suggesting the recombinant protein contains 20–40 kD of N-linked glycan. Given the peptide mass of GP1 is about 53 kD, it suggests the recombinant GP1 comprises ~12–67 kD of O-linked carbohydrate. SDS-PAGE analysis of GPΔMuc under reducing conditions revealed three major bands. The smallest band corresponding to 30–35 kD is GP2, the medium sized band of 55–70 kD is GP1 lacking mucin like domain, while the largest band represents mucin-deleted GP protein in which GP1 and GP2 were not separated, probably due to insufficient furin cleavage (Fig. 3F). The size comparison of full-length GP1 with GP1 without mucin domain indicated that the mucin-like domain is about 25–90 kD with 5–70 kD presumably from O-linked glycan.

3.3. Binding of recombinant GP1 to conformation sensitive antibodies

To assess whether conformation-dependent epitopes within GP1 are intact, we measured the binding of GP1 to mAb114, mAb100, 13C6, and their Fabs using biolayer interferometry. The Fab114 binding affinities to GP1 and GPΔMuc were found to be similar with K_Ds of 0.46 nM and 0.85 nM, respectively. Similarly, the K_Ds of Fab 13C6 for GP1 and GPΔMuc was 135 nM and 103 nM, respectively. As expected, no detectable binding was observed between GP1 and Fab100, which is specific for GP2 (Fig. 4A and B). To confirm these findings, we then captured intact mAb114, 13C6, and mAb100 antibodies onto biosensors and measured the kinetics of their binding to GP1. GP1 binds to mAb114 and 13C6 with K_Ds of 1.49 nM and 75.5 nM, respectively, and did not bind to mAb100 (Fig. 4C). Taken

together, these binding experiments demonstrated the presence of conformational epitopes for mAb114 and 13C6 on the recombinant GP1.

3.4. Binding of recombinant GP1 to DC-SIGN and DC-SIGNR

DC-SIGN and DC-SIGNR have been reported to bind Ebola virus glycoproteins [6]. However, it is not clear if the binding is through GP1. Using ELISA, we tested GP1 and GPΔMuc binding to DC-SIGN or DC-SIGNR Fc fusion proteins with human IgG1 as a control. The results showed that both GP1 and GPΔMuc bound to DC-SIGN or DC-SIGNR (Fig. 5A). This demonstrates direct recognition of DC-SIGN or DC-SIGNR by GP1 protein, and the recognition does not require the mucin-like domain. Since GPΔMuc bound to DC-SIGN and DC-SIGNR even higher than GP1, it is possible that the GP2 N-glycan may also interact with DC-SIGN/DC-SIGNR.

3.5. Cell-surface binding analysis

Many cell types, including 293T cells, are susceptible to Ebola virus infection. Others, including lymphoid cells, are resistant to Ebola virus infection [31]. To investigate if GP1 alone is sufficient for cell surface attachment, we examined biotinylated GP1 binding to SUP-T1, a lymphoblast cell line, and 293T cells using flow cytom-etry. While both SUP-T1 and 293T cells were positively stained by GP1, the protein bound 293T cells better (Fig. 5B–C). It is possible, however, that both cell lines express viral attachment factors but at different levels.

4. Discussion

Ebola is a disease with a high mortality rate but poorly understood infection mechanisms. Like other viruses, Ebola envelope proteins are the focus of therapeutic treatment and vaccine development. However, the production of recombinant GP1 has been difficult due to technical issues resulting in low expression levels. In an effort to prepare more Ebola virus GP1 protein for functional and structural studies, we made a construct containing an optimized GP1 coding gene. The optimization was based on the idea that native virus GP1 gene may not be optimal for high level expression. The results showed that optimization significantly enhanced GP1 production and the purified protein was folded similarly to native GP protein.

Codon optimization to adjust open reading frame GC content and reduce rare codon usage is a common practice in recombinant protein expression. While codon optimization intends to destabilize secondary structures present in RNA transcripts and thereby to facilitate ribosomal binding to mRNA, codon optimized genes do not always result in higher protein expression, suggesting a more complicated mechanism regulating recombinant gene expressions. Here, codon optimized GP1 expressed better than its native sequence. In addition to regular hairpin stem-loop structures, RNA also forms stable tertiary structures, known as pseudoknots [32–35]. They are formed by addition of an adjacent single strand complementary RNA to a regular hairpin stem region forming a triple-stranded stable RNA helix. Pseudoknots are known to induce ribosome pause during translational elongation and is commonly used to produce frame shift and translation of multiple viral proteins from

single mRNA [36,37]. The effect of coding region RNA pseudoknots on recombinant protein expression, however, has not been studied. To address if potential pseudoknots are present in the beginning of the open reading region to interfere ribosomal initiation, we calculated the predicted pseudoknots in the first 100 nucleotides of translational initiation site [38,39]. Interestingly, the first 100 nucleotides of the native GP1 sequence contains two predicted pseudoknots (nucleotides involved in pseudoknots are shown in yellow) (Fig. 6). In contrast, the optimized sequence contains only regular RNA hairpin stem-loops (Fig. 6, nucleotides involved in hairpin stem-loop structures are shown in blue). While this is not a proof that pseudoknots contribute to the lower expression of non-optimized GP1, it is intriguing to speculate that the presence of potential pseudoknots near the ribosomal binding and translational initiation sites may either seclude the region from ribosome or kinetically inhibit ribosome binding and thus lower the translational efficiency. As GC base pairing is favored for pseudoknot formation, a codon optimization targeted at minimize GC contents would also lower the potential of pseudoknot formation in mRNA.

Gene optimization has been widely used to achieve a better yield of recombinant protein production and here we provide another successful example. More importantly, this strategy may also be used for other difficult virus envelope protein expression.

DC-SIGN and DC-SIGNR have been implicated as Ebola virus attachment receptors. Using purified GP1 protein, we showed, for the first time, the presence of direct interactions between GP1 and DC-SIGN or DC-SIGNR. Undoubtedly, the purified GP1 protein will also be very useful for evaluation of other reported receptors as well as for the search of new receptors. It is interesting to note that large portions of sequence are shared between GP1 and sGP, which originate from the same gene [40]. The N-terminal 295 amino acids of the two proteins are identical with distinct C-terminal regions because of transcriptional editing. Although sGP forms a homo-dimer and is structurally and functionally distinct from the envelope GP1 [41], these two proteins may bear same antibody epitopes and coordinate in the pathogenesis of Ebolavirus infection. For example, antibodies elicited during infection that cross-react to sGP and GP can potentially be absorbed by sGP [42], which may prevent effective neutralization of the virus during Ebola virus infection. The purified GP1 may therefore also be used as a comparison for the research of sGP function.

Acknowledgments

This research was supported by the Intramural Research Program of the National Institutes of Health, National Institute of Allergy and Infectious Diseases. We thank Matthew Spencer for help with the manuscript.

References

1. de La Vega MA, Wong G, Kobinger GP, Qiu X. The multiple roles of sGP in Ebola pathogenesis. Viral Immunol. 2015; 28:3–9. [PubMed: 25354393]
2. Borchert M, Mutyaba I, Van Kerkhove MD, Lutwama J, Luwaga H, Bisoborwa G, Turyagaruka J, Pirard P, Ndayimirije N, Roddy P, Van Der Stuyft P. Ebola haemorrhagic fever outbreak in Masindi District, Uganda: outbreak description and lessons learned. BMC Infect Dis. 2011; 11:357. [PubMed: 22204600]

3. Trad MA, Naughton W, Yeung A, Mazlin L, O'Sullivan M, Gilroy N, Fisher DA, Stuart RL. Ebola virus disease: an update on current prevention and management strategies. J Clin Virology official Publ Pan Am Soc Clin Virology. 2016; 86:5–13.
4. Geisbert TW, Hensley LE, Larsen T, Young HA, Reed DS, Geisbert JB, Scott DP, Kagan E, Jahrling PB, Davis KJ. Pathogenesis of Ebola hemorrhagic fever in cynomolgus macaques: evidence that dendritic cells are early and sustained targets of infection. Am J pathol. 2003; 163:2347–2370. [PubMed: 14633608]
5. Alvarez CP, Lasala F, Carrillo J, Muniz O, Corbi AL, Delgado R. C-type lectins DC-SIGN and L-SIGN mediate cellular entry by Ebola virus in cis and in trans. J Virology. 2002; 76:6841–6844. [PubMed: 12050398]
6. Simmons G, Reeves JD, Grogan CC, Vandenberghe LH, Baribaud F, Whitbeck JC, Burke E, Buchmeier MJ, Soilleux EJ, Riley JL, Doms RW, Bates P, Pohlmann S. DC-SIGN and DC-SIGNR bind Ebola glycoproteins and enhance infection of macrophages and endothelial cells. Virology. 2003; 305:115–123. [PubMed: 12504546]
7. Chan SY, Empig CJ, Welte FJ, Speck RF, Schmaljohn A, Kreisberg JF, Goldsmith MA. Folate receptor-alpha is a cofactor for cellular entry by Marburg and Ebola viruses. Cell. 2001; 106:117–126. [PubMed: 11461707]
8. Quinn K, Brindley MA, Weller ML, Kaludov N, Kondratowicz A, Hunt CL, Sinn PL, McCray PB Jr, Stein CS, Davidson BL, Flick R, Mandell R, Staplin W, Maury W, Chiorini JA. Rho GTPases modulate entry of Ebola virus and vesicular stomatitis virus pseudotyped vectors. J Virology. 2009; 83:10176–10186. [PubMed: 19625394]
9. Takada A, Watanabe S, Ito H, Okazaki K, Kida H, Kawaoka Y. Down-regulation of beta1 integrins by Ebola virus glycoprotein: implication for virus entry. Virology. 2000; 278:20–26. [PubMed: 11112476]
10. Shimojima M, Takada A, Ebihara H, Neumann G, Fujioka K, Irimura T, Jones S, Feldmann H, Kawaoka Y. Tyro3 family-mediated cell entry of Ebola and Marburg viruses. J Virology. 2006; 80:10109–10116. [PubMed: 17005688]
11. Kondratowicz AS, Lennemann NJ, Sinn PL, Davey RA, Hunt CL, Moller-Tank S, Meyerholz DK, Rennert P, Mullins RF, Brindley M, Sandersfeld LM, Quinn K, Weller M, McCray PB Jr, Chiorini J, Maury W. T-cell immunoglobulin and mucin domain 1 (TIM-1) is a receptor for Zaire Ebolavirus and Lake Victoria Marburgvirus. Proc Natl Acad Sci U S A. 2011; 108:8426–8431. [PubMed: 21536871]
12. O'Hearn A, Wang M, Cheng H, Lear-Rooney CM, Koning K, Rumschlag-Booms E, Varhegyi E, Olinger G, Rong L. Role of EXT1 and glycosaminoglycans in the early stage of filovirus entry. J Virology. 2015; 89:5441–5449. [PubMed: 25741008]
13. Jae LT, Brummelkamp TR. Emerging intracellular receptors for hemorrhagic fever viruses. Trends Microbiol. 2015; 23:392–400. [PubMed: 26004032]
14. Miller EH, Chandran K. Filovirus entry into cells - new insights. Curr Opin Virology. 2012; 2:206–214.
15. Sanchez A, Trappier SG, Mahy BW, Peters CJ, Nichol ST. The virion glycoproteins of Ebola viruses are encoded in two reading frames and are expressed through transcriptional editing. Proc Natl Acad Sci U S A. 1996; 93:3602–3607. [PubMed: 8622982]
16. Bockamp EO, Fordham JL, Gottgens B, Murrell AM, Sanchez MJ, Green AR. Transcriptional regulation of the stem cell leukemia gene by PU.1 and Elf-1. J Biol Chem. 1998; 273:29032–29042. [PubMed: 9786909]
17. Lee MS, Lebeda FJ, Olson MA. Fold prediction of VP24 protein of Ebola and Marburg viruses using de novo fragment assembly. J Struct Biol. 2009; 167:136–144. [PubMed: 19447180]
18. Sanchez A, Yang ZY, Xu L, Nabel GJ, Crews T, Peters CJ. Biochemical analysis of the secreted and virion glycoproteins of Ebola virus. J Virology. 1998; 72:6442–6447. [PubMed: 9658086]
19. Cote M, Misasi J, Ren T, Bruchez A, Lee K, Filone CM, Hensley L, Li Q, Ory D, Chandran K, Cunningham J. Small molecule inhibitors reveal Niemann-Pick C1 is essential for Ebola virus infection. Nature. 2011; 477:344–348. [PubMed: 21866101]
20. Jeffers SA, Sanders DA, Sanchez A. Covalent modifications of the Ebola virus glycoprotein. J Virology. 2002; 76:12463–12472. [PubMed: 12438572]

21. Reynard O, Borowiak M, Volchkova VA, Delpeut S, Mateo M, Volchkov VE. Ebolavirus glycoprotein GP masks both its own epitopes and the presence of cellular surface proteins. J Virology. 2009; 83:9596–9601. [PubMed: 19587051]
22. Francica JR, Varela-Rohena A, Medvec A, Plesa G, Riley JL, Bates P. Steric shielding of surface epitopes and impaired immune recognition induced by the Ebola virus glycoprotein. PLoS Pathog. 2010; 6:e1001098. [PubMed: 20844579]
23. Lee JE, Fusco ML, Hessell AJ, Oswald WB, Burton DR, Saphire EO. Structure of the Ebola virus glycoprotein bound to an antibody from a human survivor. Nature. 2008; 454:177–182. [PubMed: 18615077]
24. Wang H, Shi Y, Song J, Qi J, Lu G, Yan J, Gao GF. Ebola viral glycoprotein bound to its endosomal receptor niemann-pick C1. Cell. 2016; 164:258–268. [PubMed: 26771495]
25. Kemp CW. Comparison of two methods for the transient expression and purification of Ebola glycoprotein from HEK-293 and CHO cells, in: Presented at The Essential Protein Engineering Summit, 2015. Boston, MA. 2015
26. Wilson JA, Hevey M, Bakken R, Guest S, Bray M, Schmaljohn AL, Hart MK. Epitopes involved in antibody-mediated protection from Ebola virus. Science. 2000; 287:1664–1666. [PubMed: 10698744]
27. Misasi J, Gilman MS, Kanekiyo M, Gui M, Cagigi A, Mulangu S, Corti D, Ledgerwood JE, Lanzavecchia A, Cunningham J, Muyembe-Tamfun JJ, Baxa U, Graham BS, Xiang Y, Sullivan NJ, McLellan JS. Structural and molecular basis for Ebola virus neutralization by protective human antibodies. Science. 2016; 351:1343–1346. [PubMed: 26917592]
28. Corti D, Misasi J, Mulangu S, Stanley DA, Kanekiyo M, Wollen S, Ploquin A, Doria-Rose NA, Staupe RP, Bailey M, Shi W, Choe M, Marcus H, Thompson EA, Cagigi A, Silacci C, Fernandez-Rodriguez B, Perez L, Sallusto F, Vanzetta F, Agatic G, Cameroni E, Kisalu N, Gordon I, Ledgerwood JE, Mascola JR, Graham BS, Muyembe-Tamfun JJ, Trefry JC, Lanzavecchia A, Sullivan NJ. Protective monotherapy against lethal Ebola virus infection by a potently neutralizing antibody. Science. 2016; 351:1339–1342. [PubMed: 26917593]
29. Murin CD, Fusco ML, Bornholdt ZA, Qiu X, Olinger GG, Zeitlin L, Kobinger GP, Ward AB, Saphire EO. Structures of protective antibodies reveal sites of vulnerability on Ebola virus. Proc Natl Acad Sci U S A. 2014; 111:17182–17187. [PubMed: 25404321]
30. Pallesen J, Murin CD, de Val N, Cottrell CA, Hastie KM, Turner HL, Fusco ML, Flyak AI, Zeitlin L, Crowe JE, Andersen KG, Saphire EO, Ward AB. Structures of Ebola virus GP and sGP in complex with therapeutic antibodies. Nat Microbiol. 2016; 1
31. Wool-Lewis RJ, Bates P. Characterization of Ebola virus entry by using pseudotyped viruses: identification of receptor-deficient cell lines. J Virology. 1998; 72:3155–3160. [PubMed: 9525641]
32. Staple DW, Butcher SE. Pseudoknots: RNA structures with diverse functions. PLoS Biol. 2005; 3:e213. [PubMed: 15941360]
33. Egli M, Minasov G, Su L, Rich A. Metal ions and flexibility in a viral RNA pseudoknot at atomic resolution. Proc Natl Acad Sci U S A. 2002; 99:4302–4307. [PubMed: 11904368]
34. Cash DD, Cohen-Zontag O, Kim NK, Shefer K, Brown Y, Ulyanov NB, Tzfati Y, Feigon J. Pyrimidine motif triple helix in the Kluyveromyces lactis telomerase RNA pseudoknot is essential for function in vivo. Proc Natl Acad Sci U S A. 2013; 110:10970–10975. [PubMed: 23776224]
35. Kim NK, Zhang Q, Zhou J, Theimer CA, Peterson RD, Feigon J. Solution structure and dynamics of the wild-type pseudoknot of human telomerase RNA. J Mol Biol. 2008; 384:1249–1261. [PubMed: 18950640]
36. Brierley I, Gilbert RJ, Pennell S. RNA pseudoknots and the regulation of protein synthesis. Biochem Soc Trans. 2008; 36:684–689. [PubMed: 18631140]
37. Michiels PJ, Versleijen AA, Verlaan PW, Pleij CW, Hilbers CW, Heus HA. Solution structure of the pseudoknot of SRV-1 RNA, involved in ribosomal frameshifting. J Mol Biol. 2001; 310:1109–1123. [PubMed: 11501999]
38. Sperschneider J, Datta A. DotKnot: pseudoknot prediction using the probability dot plot under a refined energy model. Nucleic acids Res. 2010; 38:e103. [PubMed: 20123730]
39. Byun Y, Han K. PseudoViewer3: generating planar drawings of large-scale RNA structures with pseudoknots. Bioinformatics. 2009; 25:1435–1437. [PubMed: 19369500]

40. Basler CF. A novel mechanism of immune evasion mediated by Ebola virus soluble glycoprotein. Expert Rev anti-infective Ther. 2013; 11:475–478.

41. Falzarano D, Krokhin O, Wahl-Jensen V, Seebach J, Wolf K, Schnittler HJ, Feldmann H. Structure-function analysis of the soluble glycoprotein, sGP, of Ebola virus. Chembiochem a Eur J Chem Biol. 2006; 7:1605–1611.

42. Pallesen J, Murin CD, Val N de, Cottrell CA, Hastie KM, Turner HL, Fusco ML, Flyak AI, Zeitlin L, Crowe JE Jr, Andersen KG, Saphire EO, Ward AB. Structures of Ebola virus GP and sGP in complex with therapeutic antibodies. Nat Microbiol. 2016; 1:16128. [PubMed: 27562261]

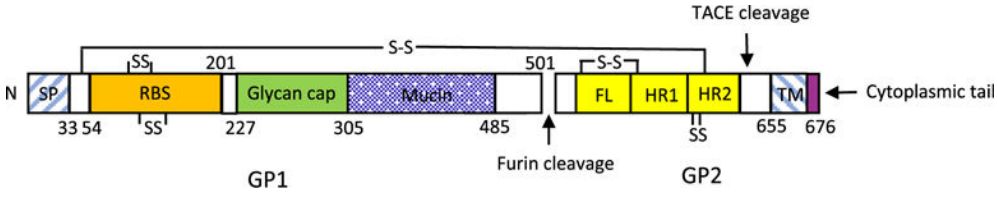

Fig. 1.

Schematic representation of Ebola virus GP. SP, signal peptide; RBS, putative receptor-binding sequence; Mucin, mucin-like domain; FL, internal fusion loop; HR1, heptad repeat 1; HR2, heptad repeat 2; TM, transmembrane domain. Lines and ‘SS’ indicate intrasubunit and intersubunit disulfide bonds; numbers represent amino acid residues.

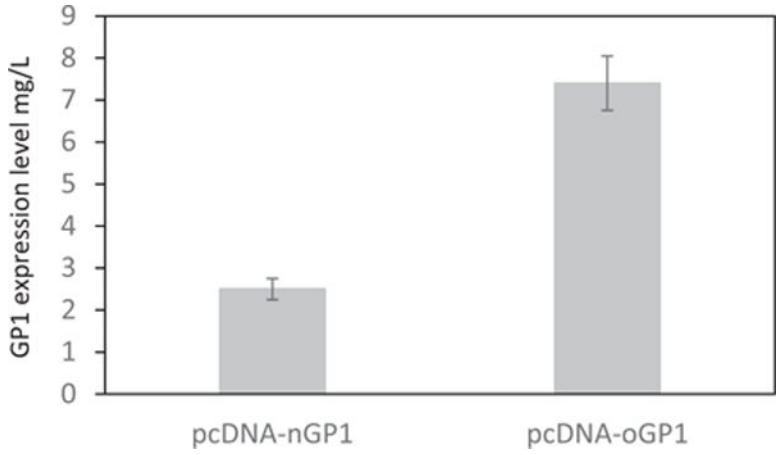

Fig. 2.

Transient expression levels of GP1. pcDNA-nGP1 and pcDNA-oGP1 were transfected into 293T cells using FuGENE® HD Transfection Reagent. One week later, culture supernatant was collected and assayed for GP1 concentration by ELISA.

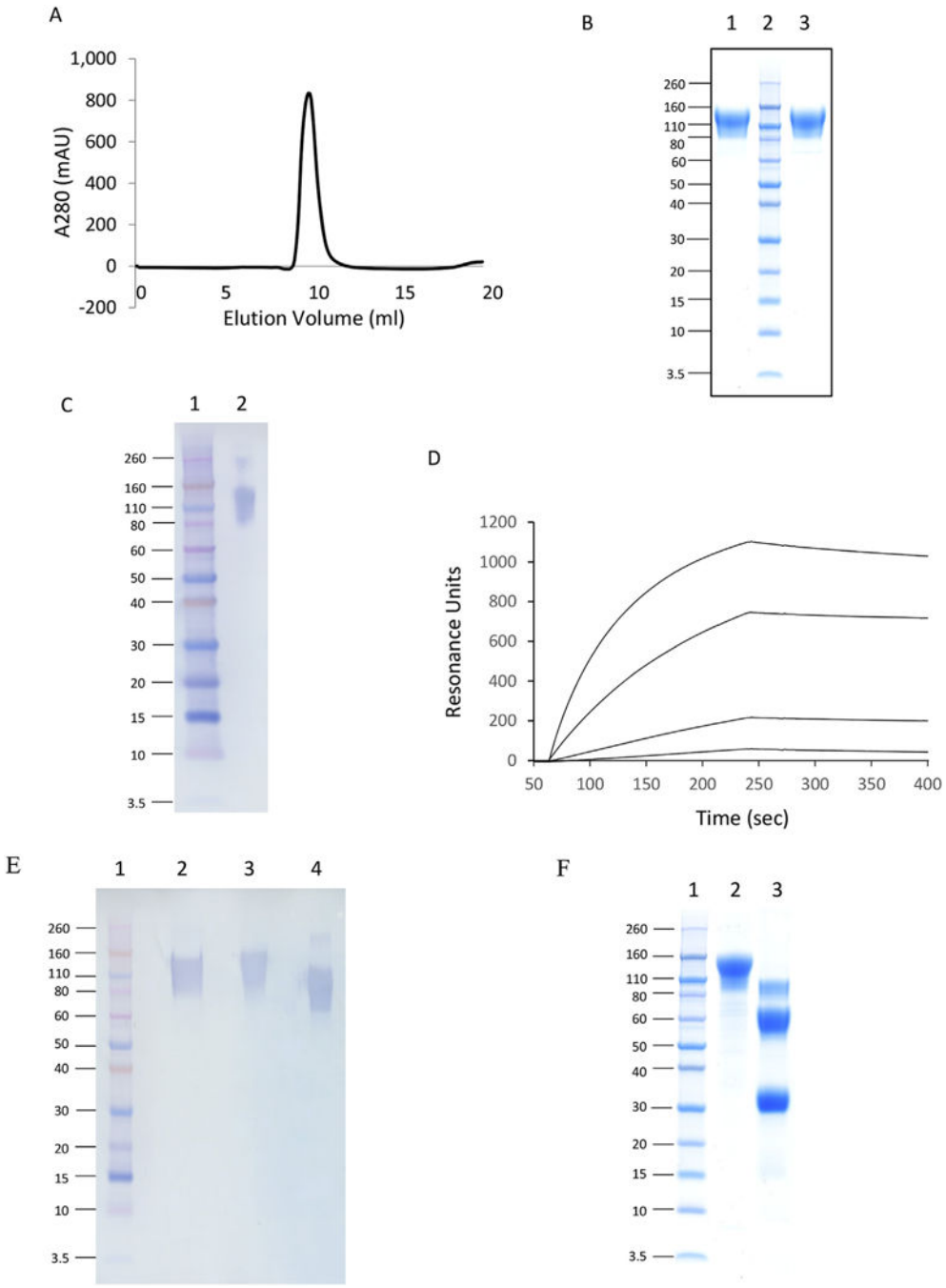

Fig. 3.

Characterization of GP1 protein purified by Ni column. A) Size exclusion chromatography elution profile. GP1 protein sample was loaded onto a Superdex 200 HR 10/30 column with PBS as a running buffer. B) SDS-PAGE analysis. GP1 samples were loaded onto a 4–12% Bis-Tris protein gel and stained with ProBlue. Lane 1, nonreducing conditions; Lane 2, protein markers; Lane 3, reducing conditions. C) Western blot analysis. 0.5 μg of purified GP1 was electrophoresed on a 4–12% SDS-polyacrylamide gel, transferred by electroblotting to a PVDF membrane, and visualized by immunostaining as described in the

text. Under nonreducing conditions: Lane 1, protein markers; Lane 2, purified GP1. D) BIAcore binding sensorgram between GP1 and mouse anti-Zaire GP monoclonal antibody. The antibody was immobilized on a CM5 chip and GP1 served as an analyte. The concentrations of GP1 was 40, 5, 0.625 and 0.078 μg/ml respectively. E) Western blot analysis of GP1 deglycosylation. Under reducing conditions: Lane 1, protein markers; Lane 2, neuraminidase treated GP1; Lane 3, untreated GP1; Lane 4, PNGase F treated GP1. F) SDS-PAGE analysis of GP1 (Lane 2) and GPΔMuc (Lane 3) under reducing conditions. Lane 1, protein markers.

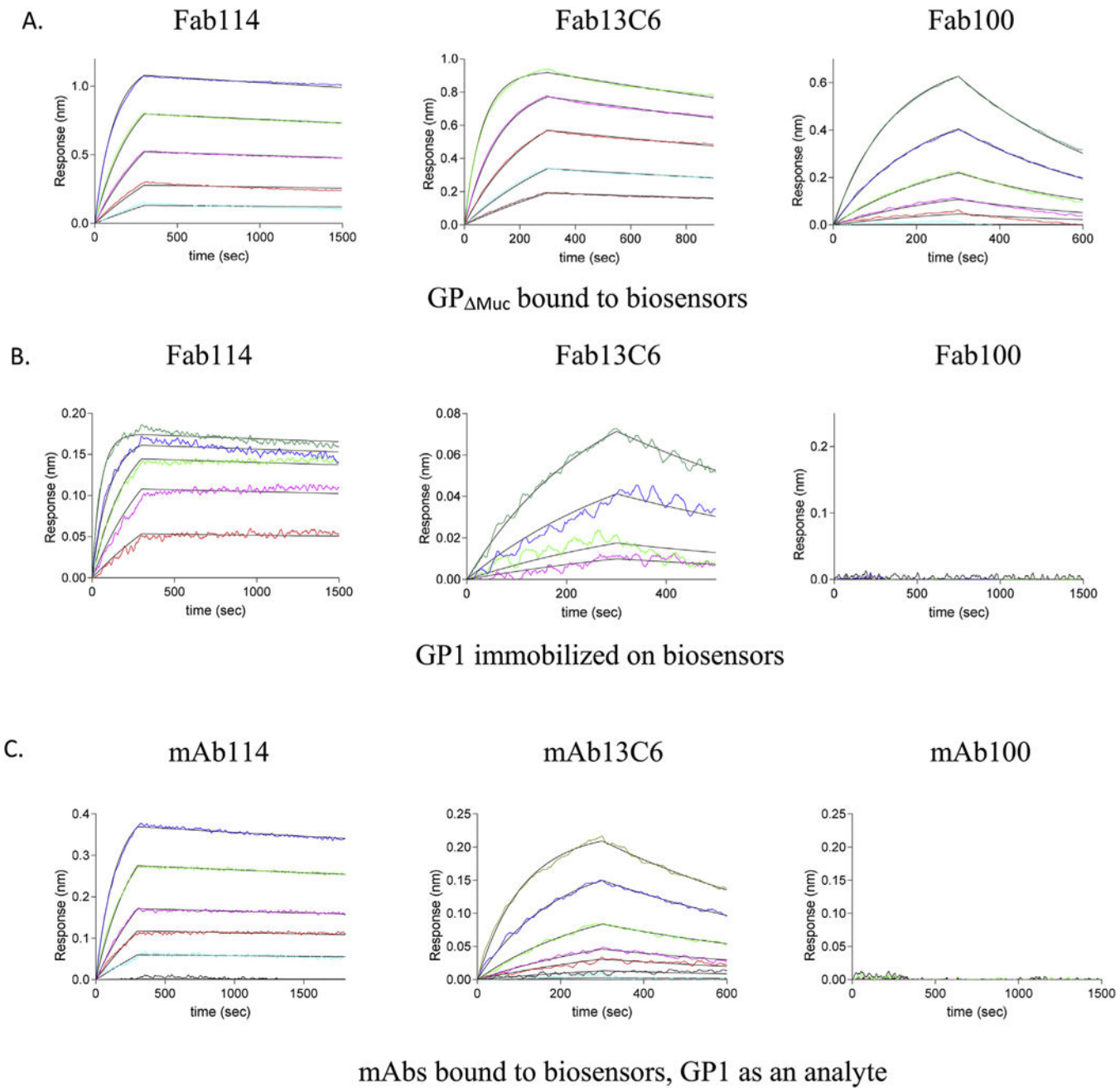

Fig. 4.

Binding kinetics of Ebola specific antibodies to GP1 protein. Biolayer interferometry (BLI) was used to determine the kinetics of binding of conformational dependent Ebola-specific antibodies mAb114, 13C6, and mAb100. A) GPΔMuc was bound to biosensors and fragment antigen-binding (Fab) fragments of mAb114 (100, 50, 25, 12.5 and 6.25 nM, respectively), 13C6 (200, 100, 50, 25, 12.5 and 6.25 nM, respectively), and mAb100 (50, 25, 12.5, 6.25 and 3.13 nM, respectively) were used as analytes. B) Purified GP1 was amine coupled to biosensors and Fab114 (200, 100, 50, 25, and 12.5 nM, respectively), Fab13C6 (200, 100, 50 and 25 nM, respectively) and Fab100 (200, 100, 50, 25, 12.5 and 6.25 nM,

respectively) were used as analytes. C) Monoclonal antibodies mAb114, mAb13C6 and mAb100 were bound to anti-human Fc biosensors and GP1 protein (200, 100, 50, 25, 12.5 and 6.25 nM, respectively for mAb114, and 400, 200, 100, 50, 25, 12.5 and 6.25 nM, respectively, for mAb13C6 and mAb100) was used as an analyte.

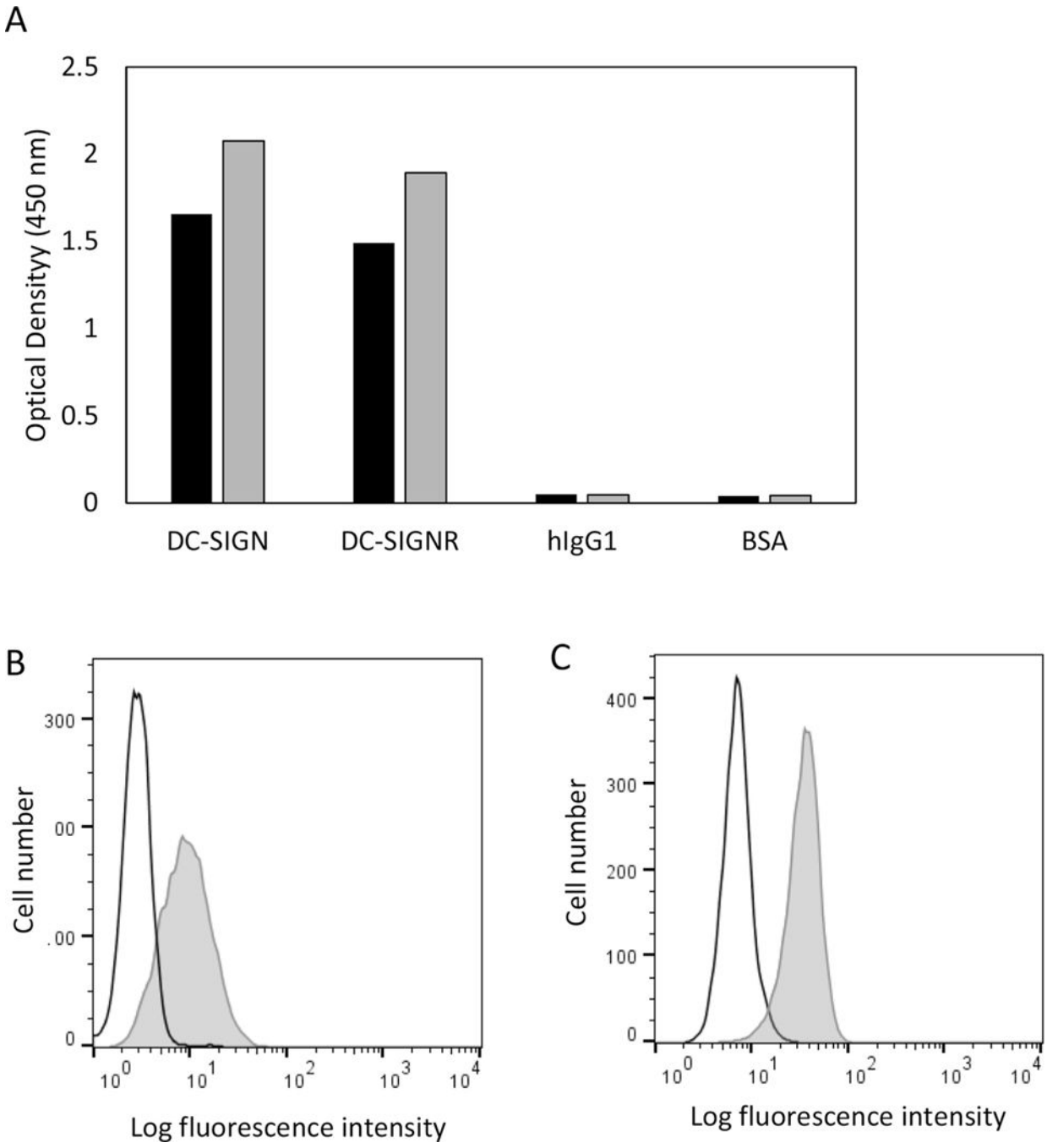

Fig. 5.

A) Binding of DC-SIGN and DC-SIGNR to GP1 and GPΔMuc. One μg of GP1 (black bar) or GPΔMuc (grey bar) was immobilized on an ELISA plate. After blocking, 1 μg of DC-SIGN-Fc, DC-SIGNR-Fc or human IgG1 was added for detection, followed by horseradish peroxidase-conjugated mouse anti-human IgG Fc antibody. BSA was used as a blank control. B–C) Binding of GP1 to cell surface. SUP-T1 (B) or HEK293T (C) cells were incubated with (grey histogram) or without (open histogram) biotinylated GP1 for 30 min on ice. After washing, cells were stained with PE-labeled streptavidin.

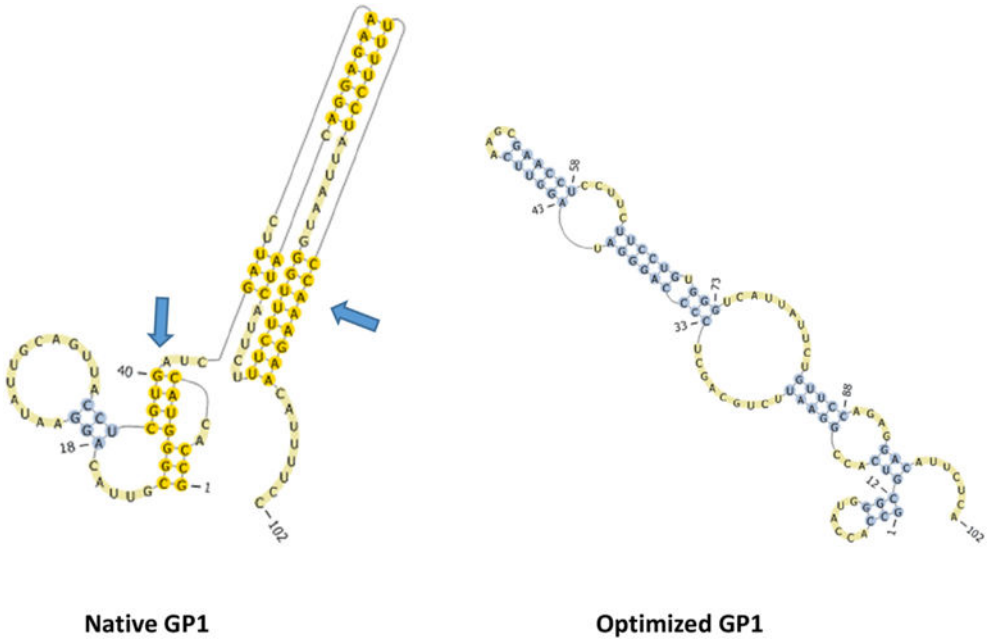

Fig. 6.

Potential RNA pseudoknots present in the first 100 nucleotides of the native but not optimized GP1 open reading frame. The two native pseudoknots are indicated by arrow. The presence of RNA pseudoknots are predicted using DOTKNOT program (http://dotknot.csse.uwa.edu.au/) and visualized by PSEUDOVIEWER (http://pseudoviewer.inha.ac.kr/).